Palladium and iridium complexes with a *N*,*P*,*N*-bis(pyridine)phenylphosphine ligand†

Shaofeng Liu,[a,b] Riccardo Peloso‡[a] and Pierre Braunstein*[a]

Received 22nd September 2009, Accepted 10th December 2009
First published as an Advance Article on the web 25th January 2010
DOI: 10.1039/b919679j

A variety of Pd(II) complexes containing the neutral *N*,*P*,*N*-ligand bis(2-picolyl)phenylphosphine ($N_{py}PN_{py}$) have been synthesised and characterized by IR and NMR spectroscopy and X-ray diffraction. The neutral complex [$PdCl_2(N_{py}PN_{py}$-*N*,*P*)] (**1**) has been selectively obtained in high yield by reaction of [$PdCl_2(NCPh)_2$] with the ligand in dichloromethane. The cationic complexes [$PdCl(N_{py}PN_{py}$-*N*,*P*,*N*)]PF_6 (**2**) and [$Pd(N_{py}PN_{py}$-*N*,*P*,*N*)(NCMe)]$(PF_6)_2$ (**5**) have been prepared from the same reagents by addition to the reaction mixture of one or two equivalents of $TlPF_6$, respectively. It was found that dynamic exchange of the pyridine rings of **1** occurs on the NMR time-scale and possible mechanisms are discussed. As a by-product of the synthesis of **2**, the unexpected dinuclear complex [$Pd_2Cl_2(\mu$-$N_{py}PN_{py})_2$]$(PF_6)_2$ (**3**) has been isolated in 10% yield. Its molecular structure in the solid state reveals the presence of two $N_{py}PN_{py}$ chelating/bridging ligands. The cationic complex [$Pd_2Cl_2(\mu$-$N_{py}PN_{py})_2$]$^{2+}$ was then selectively obtained by reaction of *cis*-[$Pd(N_{py}PN_{py}$-*N*,*P*)$_2$]$(BF_4)_2$ (**4**) with [$PdCl_2$(cod)]. ^{1}H- and ^{31}P{^{1}H} NMR studies have demonstrated that **3** converts slowly into **2** in DMSO solution. The Ir(I) complexes [IrCl(cod)($N_{py}PN_{py}$)] (**6**) and [Ir(cod)($N_{py}PN_{py}$-*N*,*P*,*N*)]BAr^F (**7**) have also been prepared, the latter exhibits a trigonal bipyramidal structure with the ligand displaying a facial coordination mode. Compound **7** represents a rare example of an Ir(I) complex bearing a *N*,*P*,*N*-chelating ligand.

Introduction

The synthesis and coordination chemistry of heterotopic ligands bearing phosphorus and nitrogen donor atoms represent increasingly active fields of research owing to the properties that such ligands confer to their metal complexes in stoichiometric or catalytic reactions.[1-11] The significantly different electronic and hard–soft properties of the donor functions largely influence their metal coordination behaviour and account for the observation of monodentate *P*- or *N*-coordination and static or dynamic (hemilabile) *P*,*N*-chelation.[2]

In the course of our studies on *P*,*N*-ligands in which the P donor function is of the phosphine, phosphonite or phosphinite-type and the N donor belongs to a pyridine or an oxazoline heterocycle, we observed that some of their mononuclear complexes of Ru(II),[6,12-15] Ni(II),[7,16,17] Co(II)[18] and Pd(II)[15,19,20] or Fe–Cu[21] and Fe–Co[22] bimetallic complexes led to active precatalysts for a number of reactions.

As an extension to *N*,*P*,*N*-tridentate ligands containing oxazoline heterocycles, we compared the bonding behaviour of the bis(oxazoline)phenylphosphine (abbreviated below for clarity as $N_{ox}PN_{ox}^{Me2}$) and bis(oxazoline)phenylphosphonite ligands (abbreviated $NOPON^{Me2}$) (Scheme 1). It was unexpectedly found that the former can behave as a *N*,*N*-chelate towards Co(II) and Fe(II),[17,23] in contrast to the situation in [$CoCl_2(NOPON^{Me2}$-*P*,*N*)][23](Scheme 1).

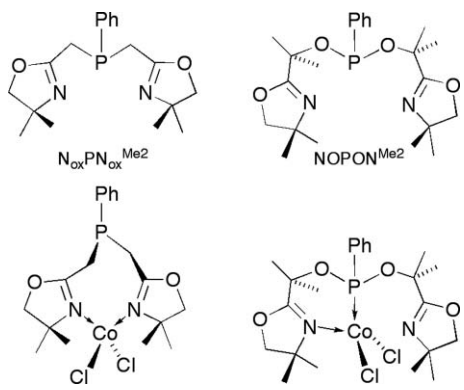

Scheme 1 The ligands $N_{ox}PN_{ox}^{Me2}$ and $NOPON^{Me2}$ and contrasting bonding modes of the heterofunctional ligands in complexes [$CoCl_2(NOPON^{Me2}$-*P*,*N*)] and [$CoCl_2(N_{ox}PN_{ox}^{Me2}$-*N*,*N*)].

As far as bis(oxazoline)phosphine ligands are concerned, only *P*,*N*- or *N*,*P*,*N*-coordination modes have been observed in Pd(II) complexes (Scheme 2).[17,23] We wished to extend these studies to the corresponding *N*,*P*,*N*-ligand where N represents a pyridine donor ($N_{py}PN_{py}$) and compare its coordination properties with those of $N_{ox}PN_{ox}^{Me2}$, in particular towards Pd(II) complexes.

[a]*Laboratoire de Chimie de Coordination, Institut de Chimie (UMR 7177 CNRS), Université de Strasbourg, 4 rue Blaise Pascal, F-67070, Strasbourg Cedex, France. E-mail: braunstein@unistra.fr*
[b]*Key Laboratory of Engineering Plastics and Beijing National Laboratory for Molecular Sciences, Institute of Chemistry, Chinese Academy of Sciences, Beijing, 100190, China*

† Electronic supplementary information (ESI) available: ORTEP plot of [$PdBr_2(N_{py}PN_{py}$-*N*,*P*)] (Fig. S1). CCDC reference numbers 748557–748562 and 757233. For ESI and crystallographic data in CIF or other electronic format see DOI: 10.1039/b919679j

‡ current address: Instituto de Investigaciones Químicas - Departamento de Química Inorgánica, Universidad de Sevilla - Consejo Superior de Investigaciones Científicas, Avda. Américo Vespucio 49, Isla de la Cartuja, 41092 Sevilla, Spain.

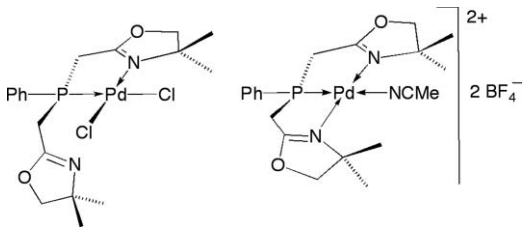

Scheme 2 The complexes $[PdCl_2(NPN^{Me2}\text{-}P,N)]$ and $[Pd(NPN^{Me2}\text{-}N,P,N)(NCMe)](BF_4)_2$.

For this purpose, the ligand selected was bis(2-picolyl)-phenylphosphine ($N_{py}PN_{py}$, Scheme 3), a flexible, symmetric and neutral *N*,*P*,*N*-ligand containing two pyridine arms and a phosphine-type P donor.[24,25] We have also performed preliminary studies on the coordination chemistry of this ligand to Ir(I) complexes, in order to investigate its behaviour with a d^8 metal which is more prone to give rise to penta-coordinated complexes. Moreover, *N*,*N*,*N*-,[26] *P*,*C*,*P*-,[27] and, very recently, *P*,*N*,*P*-Ir(I)[28] chelated complexes have proved to be effective in a number of challenging catalytic reactions and in C–H bond activation. In this context, the preparation of new *N*,*P*,*N*-chelated Ir complexes represents a desirable development of this chemistry.[29] Herein, we report the synthesis and the characterization of Pd(II) and Ir(I) complexes bearing the neutral bis(2-picolyl)phenylphosphine ($N_{py}PN_{py}$) ligand.

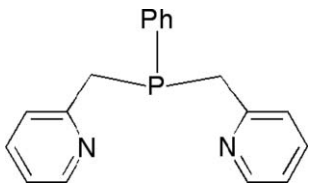

Scheme 3 The $N_{py}PN_{py}$ ligand.

Results and discussion

The reaction between $[PdCl_2(NCPh)_2]$ and an equimolar amount of $N_{py}PN_{py}$ in CH_2Cl_2 resulted in the formation of a yellow precipitate, which was characterized by multinuclear NMR and IR spectroscopy, elemental analysis and X-ray diffraction and identified as the mononuclear complex $[PdCl_2(N_{py}PN_{py}\text{-}N,P)]$ (**1**). The compound is poorly soluble in most organic solvents and only DMF and DMSO allowed us to prepare concentrated solutions of **1**. The $^{31}P\{^1H\}$ NMR spectrum of **1** in DMSO shows a sharp singlet at 49.7 ppm, thus confirming the coordination of the ligand through the phosphorus atom, whose resonance is downfield shifted by about 60 ppm with respect to the free ligand. At this point, we cannot say whether this resonance corresponds to the neutral complex or, in view of the high donor number (DN = 29.8) of DMSO,[30] to the cation of $[PdCl(N_{py}PN_{py}\text{-}N,P)(DMSO)]Cl$ which would form upon dissolution of the neutral complex in DMSO. The ^1H NMR spectrum of **1** at room temperature exhibits broad signals due to the picolyl moieties of the ligand, whereas the phenyl protons give rise to sharp signals. In particular, the presence of eight broad resonances in the pyridine region indicates the non-equivalence of the two pyridine rings, which are likely to be involved in a dynamic slow exchange of the nitrogen donors N^1 and N^2 on the NMR time scale (Scheme 4). We shall come back to this point later in the discussion.

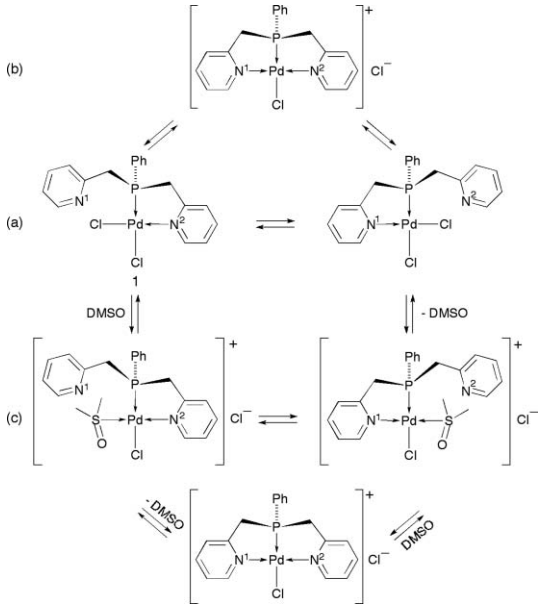

Scheme 4 Possible mechanisms for the dynamic exchange of the pyridine rings at the Pd centre in **1**.

Although it was not possible to assign all the signals in the pyridine region, by comparison with the values found for $[PdCl(N_{py}PN_{py}\text{-}N,P,N)]PF_6$ (**2**, *vide infra*), we suggest that the H *ortho* to the coordinated nitrogen in **1** resonates at 9.32 ppm and that of the non-coordinated pyridine moiety at 8.39 ppm. In order to better understand this dynamic behaviour, we performed variable temperature ^1H NMR experiments from 25 to 80 °C. The gradual broadening of the eight pyridine resonances resulted in the coalescence of the signals at 80 °C (300 MHz), which gave rise to four broad peaks at 8.89, 7.86, 7.62, 7.34 ppm. By means of a line shape analysis, the rates of exchange were estimated at different temperatures and this allowed us to calculate the following activation parameters by an Eyring plot: $\Delta H^{\ddagger} = (50 \pm 3)$ kJ mol^{-1}, $\Delta S^{\ddagger} = (-43 \pm 8)$ J mol^{-1} K^{-1}. As far as the $^{13}C\{^1H\}$ NMR spectrum of **1** is concerned, it is worth observing that the signals of the coordinated picolyl moiety (py^2, py^6, py^4 and CH_2) are downfield shifted with respect to those of the non-coordinated one. This is likely to result from a decrease of the electron-density at the pyridine ring upon coordination. The far IR spectrum of the compound displays two strong absorptions at 337 and 301 cm^{-1}, which are ascribed to the Pd–Cl stretching vibrations of the *cis*-$PdCl_2$ moiety.[31,32]

The molecular structure of **1** (Fig. 1) in the solid state confirmed that the $N_{py}PN_{py}$ ligand behaves as a bidentate *N*,*P*-chelate, one of the pyridine rings remaining non-coordinated, as also observed in the related $N_{ox}PN_{ox}$ Pd(II) complex.[23] Similarly, it has been previously observed that a hemilabile bis(oxazoline)phenylphosphonite acts as a *N*,*P*-bidentate ligand in the monohaptyl allyl complex $[Pd(\eta^1\text{-}C_3H_5)Cl(NOPON^{Me2})]$.[33] The phosphorus atom becomes a stereogenic centre upon coordination and both enantiomers are present in the unit cell. The palladium atom lies in a distorted square-planar coordination environment, as shown by the bond angles about the metal, which range from 83.29(8) (N1–Pd1–P1)

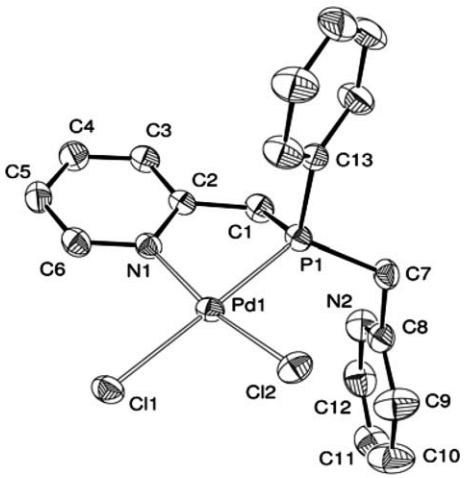

Fig. 1 ORTEP of complex **1** with ellipsoids drawn at the 50% probability level. Selected bond distances (Å) and angles (deg): Pd1–Cl1 2.3825(9), Pd1–Cl2 2.2945(9), Pd1–P1 2.200(1), Pd1–N1 2.075(3), N1–Pd1–P1 83.29(8), N1–Pd1–Cl1 94.97(8), Cl1–Pd1–Cl2 92.80(4), Cl2–Pd1–P1 89.02(4).

to 94.97(8)° (N1–Pd1–Cl1). The Pd–Cl bond distances of 2.2945(9) Å and 2.3825(9) Å, for the positions *trans* to nitrogen and *trans* to phosphorus, respectively, reflect the higher *trans* influence of the latter donor.[34] The molecular structure of the analogous complex [$PdBr_2(N_{py}PN_{py}$-*N*,*P*)] ($^{31}P\{^1H\}$ NMR: δ 49.4 ppm) was determined for comparison and is very similar to that of **1** (see ESI†).

Abstraction of a chloride anion from **1** was expected to induce a tridentate chelating behaviour of the $N_{py}PN_{py}$ ligand. The reaction was performed directly by mixing in THF the palladium complex [$PdCl_2(NCPh)_2$] with the ligand in the presence of one equivalent of $TlPF_6$, which was added after several hours. The reaction proceeded heterogeneously because of the formation first of the insoluble complex **1** and gave rise to a mixture of two complexes, which were separated by crystallization. The main-product was the expected complex [$PdCl(N_{py}PN_{py}$-*N*,*P*,*N*)]PF_6 (**2**), whereas the by-product was shown by X-ray diffraction to be the unexpected cationic dinuclear complex [$Pd_2Cl_2(\mu$-$N_{py}PN_{py})_2$]$(PF_6)_2$ (**3**). The NMR spectra of the two compounds in DMSO-d_6 at room temperature are different. In particular, the ^1H NMR spectrum of the dinuclear complex exhibits a doublet at 9.27 ppm due to two equivalent py^6 protons, whereas the py^6 protons of the mononuclear complex **2** resonate at 9.06 ppm. This allowed us to estimate the molar ratio between the mononuclear and the dinuclear complexes in the crude, which was found to be about 7/1. Although compound **3** is indefinitely stable in the solid state, we observed that it converts slowly into compound **2** in DMSO solution, the conversion being complete after 4 days at room temperature or 10 h at 80 °C. We wondered whether the formation of the dinuclear complex was due to the heterogeneous conditions of the synthesis and, consequently, we repeated the reaction under homogeneous conditions by changing the nature of the solvent (DMSO instead of THF). As expected, the addition of one equivalent of $TlPF_6$ to a DMSO-d_6 solution of **1**, which forms in the first step of the synthesis of **2** and **3**, afforded selectively the mononuclear, cationic complex **2**. The $^{31}P\{^1H\}$ NMR spectrum of pure **2** in DMSO-d_6 exhibits two broad signals at 83.7 and 56.4 ppm, which are attributed to two different cationic complexes present in solution, namely [$PdCl(N_{py}PN_{py}$-*N*,*P*,*N*)]$^+$ and a complex resulting from coordination of a DMSO molecule and displacement of a pyridine group, [$PdCl(N_{py}PN_{py}$-*N*,*P*)(DMSO)]$^+$ (Scheme 5). The intensities of the two broad resonances provide an estimate of the molar ratio between the two species in equilibrium, which is about 3 : 1 ([$PdCl(N_{py}PN_{py}$-*N*,*P*,*N*)]$^+$/[$PdCl(N_{py}PN_{py}$-*N*,*P*)(DMSO)]$^+$).

The two broad $^{31}P\{^1H\}$ NMR resonances (56.4 and 83.7 ppm) are found in the same region as those exhibited by **1** and the dicationic complex [$Pd(NCMe)(N_{py}PN_{py}$-*N*,*P*,*N*)]$(PF_6)_2$ (**5**, *vide infra*), which occurs respectively at 49.7 and 86.6 ppm in DMSO-d_6. So, it seems likely that the peak at 56.4 ppm is due to a complex where $N_{py}PN_{py}$ acts as a bidentate *N*,*P*-donor ligand, similarly to **1**, while the peak at 83.7 ppm is due to a complex where it behaves as a tridentate *N*,*P*,*N*-donor ligand, similarly to [$Pd(NCMe)(N_{py}PN_{py}$-*N*,*P*,*N*)]$(PF_6)_2$. This hypothesis is also consistent with the fact that the ^1H NMR spectrum of **2** in DMSO-d_6 shows broad signals in both the pyridine and methylene regions. This is probably caused by the exchange equilibrium of the two pyridine moieties around the palladium atom in the [$PdCl(N_{py}PN_{py}$-*N*,*P*)(DMSO)]$^+$ species, as assumed for compound **1** (see below). In the $^{13}C\{^1H\}$ NMR spectrum of **2**, two sets of signals are observed, as expected: broad resonances corresponding to the DMSO substituted species and sharp resonances due to the [$PdCl(N_{py}PN_{py}$-*N*,*P*,*N*)]$^+$ cation. The equilibrium constant for the formation of the solvento-complex in Scheme 5 (K_{eq} = [PdCl(NPN)(DMSO)]/[PdCl(NPN)]) was calculated at different temperatures, ranging from 25 to 80 °C, on the basis of the molar ratio of the two species in the ^{31}P NMR of pure **2**. Hence, the thermodynamic parameters were estimated by means of a Van't Hoff plot. The displacement of one pyridine ring by DMSO in DMSO solution was found to be slightly endothermic with $\Delta H = (8 \pm 1)$ kJ mol^{-1} and $\Delta S = (21 \pm 3)$ J mol^{-1} K^{-1}. The far IR spectrum of **2** exhibits an absorption at 343 cm^{-1}, which is likely to be due to the Pd–Cl stretching vibration, and a strong band at 556 cm^{-1} tentatively assigned to the Pd–N stretching vibration.[35]

The molecular structure of the cationic complex [$PdCl(N_{py}PN_{py}$-*N*,*P*,*N*)]$^+$ in **2**·CH_2Cl_2 is shown in Fig. 2. Its coordination geometry approximates to square-planar, the N–Pd–P angles being 83.3(1)°

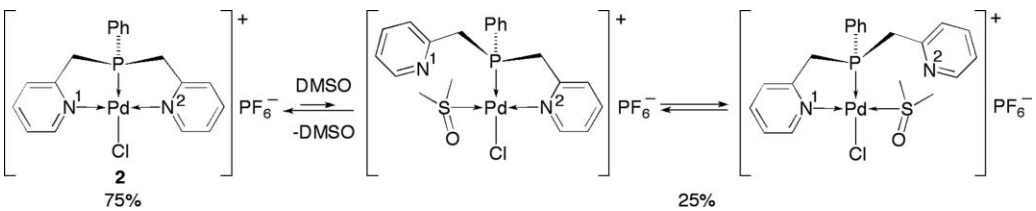

Scheme 5 Dynamic behaviour of **2** in DMSO solution.

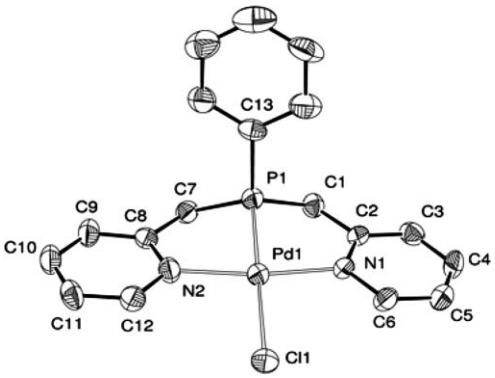

Fig. 2 ORTEP of the cationic complex in **2**·CH_2Cl_2 with ellipsoids drawn at the 50% probability level. Selected bond distances (Å) and angles (deg): Pd1–Cl1 2.388(2), Pd1–P1 2.171(2), Pd1–N1 2.057(4), Pd1–N2 2.056(4), N1–Pd1–P1 83.35(13), N2–Pd1–P1 83.71(14), N1–Pd1–Cl1 96.80(13), N2–Pd1–Cl1 96.42(14), Cl1–Pd1–P1 177.50(5).

and 83.7(1)°. There is no symmetry element in the molecule. In spite of the positive charge of the complex, the Pd–Cl bond distance of 2.388(2) Å does not differ significantly from that observed in **1** (*trans* to P). The Pd–P (2.171(2) Å) and Pd–N (2.057(4) and 2.056(4) Å) bond distances are slightly shorter than in complex **1**.

Let us now come back to the dynamic exchange involving complex **1**. It could formally occur by three different mechanisms: an associative displacement of N^2 for N^1, without chloride dissociation (Scheme 4a), chloride displacement by N^1 to give a cationic complex with a tridentate *N*,*P*,*N* ligand [PdCl($N_{py}PN_{py}$-*N*,*P*,*N*)]Cl closely related to **2** (see below) and chloride recoordination and displacement of N^2 (Scheme 4b), or dissociation of **1** in DMSO, nitrogen/DMSO exchange followed by chloride recoordination (Scheme 4c). In order to check their feasibility, we mixed equimolar amounts of **1** and **2** in an NMR tube and observed at room temperature a $^{31}P\{^1H\}$ resonance at 83.7 and a more intense and broad one at 50.3 ppm. The former corresponds to [PdCl($N_{py}PN_{py}$-*N*,*P*,*N*)]$^+$ and the latter to the overlap between those assigned to **1** (49.7 ppm) and to [PdCl($N_{py}PN_{py}$-*N*,*P*)(DMSO)]$^+$ (56.4 ppm). When the temperature was raised to 80 °C, the resonance at 83.7 ppm disappeared and the other was found at 49.1 ppm. These experiments suggest that **1** and **2** give rise to a common cationic species in solution and that the latter exchanges with **2** at higher temperature. This is consistent with a mechanism such as that shown in Scheme 4c. We verified independently that the cation in **2**, [PdCl($N_{py}PN_{py}$-*N*,*P*,*N*)]$^+$, reacts with excess (NMe_4)Cl in DMSO to give a single species, according to $^{31}P\{^1H\}$ spectroscopy, characterized by a singlet at 49.7 ppm, which is exactly the value found for **1**. Whether this is the dichloro complex or its solvento derivative (see above), this experiment demonstrates that a pyridine donor of the tridentate form of the $N_{py}PN_{py}$ ligand can be readily displaced by chloride to give a complex with a $N_{py}PN_{py}$-*N*,*P* chelate. This is again consistent with a mechanism of the type shown in Scheme 4c. When complex **2** was treated in DMSO with only half an equivalent of (NMe_4)Cl, a sharp resonance was still present at 83.8 ppm, corresponding to the complex with the tridentate $N_{py}PN_{py}$ ligand, and a broad resonance was observed at 52.3 ppm which could correspond to the complexes **1** and [PdCl($N_{py}PN_{py}$-*N*,*P*)(DMSO)]Cl in slow exchange on the NMR time-scale.

The $^{31}P\{^1H\}$ NMR spectrum of **3** in DMSO-d_6 shows a broad resonance at 47.5 ppm, whereas the ^1H NMR spectrum displays sharp signals in the aromatic region and broad signals due to the methylene protons. Consistent with the molecular structure of **3** in the solid state, the two pyridine moieties of each ligand are not equivalent. Particularly remarkable is the difference between the resonances of the protons *ortho* to the nitrogen, which is more than 1 ppm. As expected for the *trans* arrangement of the $PdCl_2$ moiety, the far IR spectrum of **3** contains only one absorption at 346 cm^{-1} for the Pd–Cl stretching vibration.[31]

The solid-state structure of **3** deserves a more detailed description. It is shown in Fig. 3.

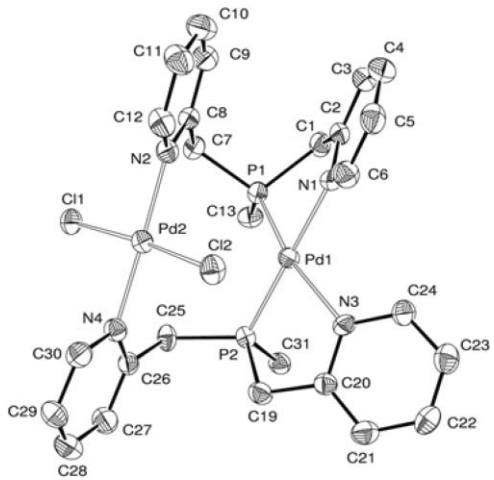

Fig. 3 ORTEP of the dinuclear cationic complex in **3**·2(CH_2Cl_2) with ellipsoids drawn at the 50% probability level. Only the *ipso* carbons of the P-phenyl groups are shown for clarity. Selected bond distances (Å) and angles (deg): Pd1–P1 2.224(1), Pd1–P2 2.242(1), Pd1–N1 2.116(3), Pd1–N3 2.123(3), Pd2–Cl1 2.315(1), Pd2–Cl2 2.301(1), Pd2–N2 2.047(3), Pd2–N4 2.020(3), N1–Pd1–P1 81.85(9), N3–Pd1–P2 82.08(9), N4–Pd2–N2 177.0(1), Cl2–Pd2–Cl1 174.95(4).

The cationic complex (Fig. 3) consists of two square-planar palladium units linked by two bridging $N_{py}PN_{py}$ ligands, which *P*,*N*-chelate one palladium centre (Pd1) and act as N donor ligands towards the other one (Pd2). The coordination environment of Pd2 is completed by two chlorides in *trans* position to each other. Thus, this dinuclear dicationic complex features an unusual charge differentiation between the two metal centres, Pd1 formally carrying the doubly positive charge and the Pd2 moiety being neutral.

The coordination geometry around Pd1 shows a pronounced distortion from planarity, the P1–Pd2–N3 angle being 161.4(1)°, significantly smaller than the related P2–Pd1–N1 of 179.0(1)°. The angle between the two mean coordination planes, defined by the atoms Pd1,P1,P2,N1,N3 and Pd2,Cl1,Cl2,N4,N2 is 13.09(4)°. The phosphorus atoms become stereogenic centres upon coordination and exhibit opposite configurations, the resulting isomer being the *meso* diastereoisomer. The Pd2–Cl bond distances are in the usual range and the Pd1–N bond distances are affected by the *trans* influence of the phosphine and are significantly longer than the Pd2–N bond distances.[34] A similar coordination behaviour

of the $N_{py}PN_{py}$ ligand has been recently observed in the Ag(I) complex $[Ag(N_{py}PN_{py})]_2(BF_4)_2$[24] in which the two metal centres are additionally linked by an Ag–Ag bond.

The unexpected structure of **3** prompted us to develop a more straightforward and selective synthesis of this compound. Looking at the different coordination environments of the two palladium centres in **3**, it seemed convenient to first prepare a dicationic complex bearing two $N_{py}PN_{py}$ ligands, and then react this complex with a Pd(II) precursor containing the $PdCl_2$ fragment. The reaction between $[Pd(NCMe)_4](BF_4)_2$ and $N_{py}PN_{py}$ in a 1 : 2 molar ratio in dichloromethane afforded a pale yellow solid, which was identified by spectroscopy and X-ray diffraction as the mononuclear complex *cis*-$[Pd(N_{py}PN_{py}\text{-}N,P)_2](BF_4)_2$ (**4**).

In the molecular structure of **4**·2(CH_2Cl_2) (Fig. 4), a C_2 symmetry axis passes through the metal atom and the middle points of the P···P and N···N segments. The phosphorus atoms thus display the same configuration and the complex is consequently chiral. Both enantiomers are present in the unit cell. As expected, the Pd–P and Pd–N bond distances in **4** (2.229(1) and 2.108(3) Å, respectively) are very similar to those observed in **3**. Compound **4** was reacted in DMSO-d_6 with an equimolar amount of [$PdCl_2$(cod)]. The ^{1}H- and $^{31}P\{^1H\}$ NMR spectra of the resulting solution revealed the selective formation of the dinuclear cationic complex $[Pd_2Cl_2(\mu\text{-}N_{py}PN_{py})_2]^{2+}$ of **3** (Scheme 6).

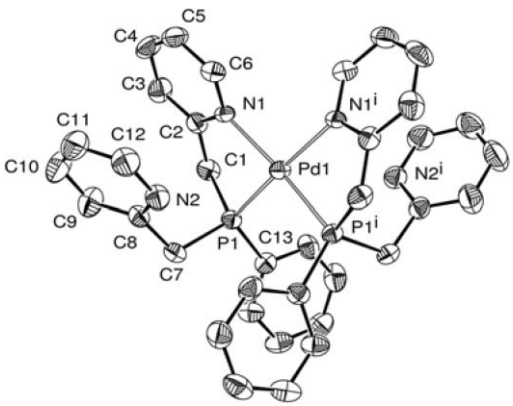

Fig. 4 ORTEP of the cationic complex in **4**·2(CH_2Cl_2) with ellipsoids drawn at the 50% probability level. Selected bond distances (Å) and angles (deg): Pd1–N1 2.108(3), Pd1–P1 2.229(1), N1–Pd1–$N1^i$ 98.4(2), N1–Pd1–P1 82.21(9), P1–Pd1–$P1^i$ 98.65(6). Symmetry operation generating equivalent atoms (^{i}): −x, y, −z.

Furthermore, the synthesis of a dicationic Pd(II) complex containing the $N_{py}PN_{py}$ ligand was realized by extracting both chloride anions from the coordination sphere of the metal. Thus, the one-pot 1 : 1 reaction between $[PdCl_2(NCPh)_2]$ and the $N_{py}PN_{py}$ in the presence of two equivalents of $TlPF_6$ in MeCN afforded selectively a pale yellow compound in high yield, which was identified as the expected complex $[Pd(N_{py}PN_{py}\text{-}N,P,N)(NCMe)](PF_6)_2$ (**5**).

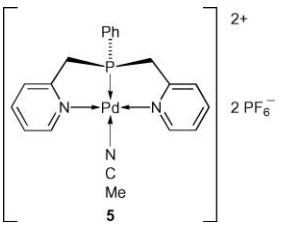

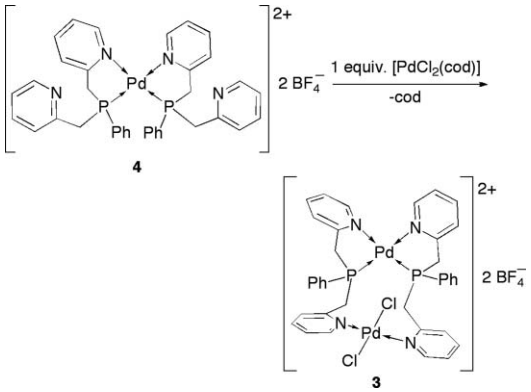

Scheme 6 Selective formation of **3** from **4** and [$PdCl_2$(cod)].

As far as the NMR spectra of **5** in DMSO are concerned, the main difference to be noted with respect to compounds **1–3** is the absence of broad signals. Moreover, the picolyl moieties are equivalent as proved by the ^{1}H and $^{13}C\{^1H\}$ NMR spectra. These observations are consistent with a tridentate coordination behaviour of the ligand, where the pyridine moieties are strongly bound to the metal and not displaced by the DMSO, at variance with the situation suggested for compound **2**. Nevertheless, the displacement of the acetonitrile by a dimethylsulfoxide molecule was established by the presence of the signals of free acetonitrile in both ^{1}H- and $^{13}C\{^1H\}$ NMR spectra. The $^{31}P\{^1H\}$ NMR spectrum of **5** displays a sharp singlet at 86.6 ppm. The difference between this value and that observed for **2** is only 3.3 ppm and suggests that the phosphorus nuclei in the two complexes lie in a very similar electronic environment. The increase of the formal charge of the cationic complex from +1 (for **2**) to +2 (for **5**) does not affect significantly the chemical shift of the phosphorus atom but causes, as expected, a slight downfield shift. As anticipated, the ^{1}H NMR of **5** in DMSO-d_6 displays only sharp signals. The ABX spin system for the CH_2P protons was expected to give rise to two doublet of doublets ($^2J_{HH}$, and two $^2J_{PH}$). In fact, two triplets are observed in the methylene region, thus suggesting that the $^2J_{PH}$ are very similar to the $^2J_{HH}$. The ABX spin system could be converted into an AB spin system by recording the $^1H\{^{31}P\}$ NMR spectrum of **5**, which showed two doublets at 5.21 and 4.29 ppm with $^2J_{HH}$ = 17.7 Hz. In the far IR spectrum of **5**, the Pd–N stretching vibration causes a strong absorption at 554 cm^{-1}.[35] A view of the molecular structure of the cationic complex in **5**·MeCN is depicted in Fig. 5. Bond distances and angles in the $Pd(N_{py}PN_{py})$ fragment are in most cases identical to those observed in **2**·CH_2Cl_2, the main difference being a shorter Pd–P distance in **5**. This is probably due to the decrease in the overall charge of cation from +1 (in **2**) to +2 (in **5**).

It appeared interesting to extend our study of the $N_{py}PN_{py}$ ligand to another d^8 transition metal system. Since it was previously reported that $N_{py}PN_{py}$ acts as a facial tridentate ligand in octahedral Fe(II)[17] and Cr(III)[36] complexes, we wondered which type of coordination geometry would have been obtained for a metal cation that can have either a square planar or a trigonal bipyramidal coordination environment. Ir(I) was expected to be a good candidate for this purpose. Moreover, although the chemistry of iridium complexes containing tridentate ligands such as *P*,*C*,*P*-pincer[27] or tris(pyrazolyl)borate ligands[26] has been extensively studied, to the best of our knowledge, only two structurally

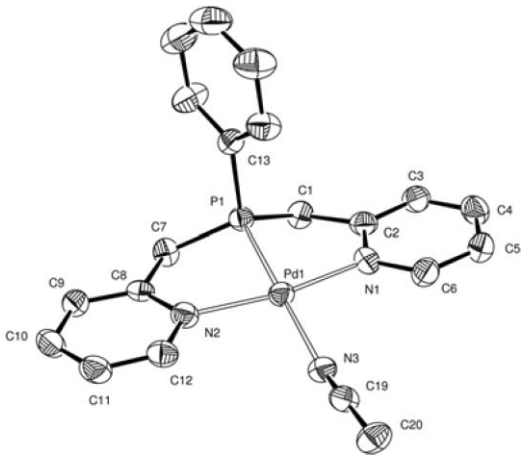

Fig. 5 ORTEP of the cationic complex in **5**·MeCN with ellipsoids drawn at the 50% probability level. Selected bond distances (Å) and angles (deg): Pd1–P1 2.163(1), Pd1–N1 2.063(4), Pd1–N2 2.051(4), Pd1–N3 2.125(4), N1–Pd1–P1 83.4(1), N2–Pd1–P1 82.6(1), N1–Pd1–N3 97.0(2), N2–Pd1–N3 97.1(2), N3–Pd1–P1 178.1(1).

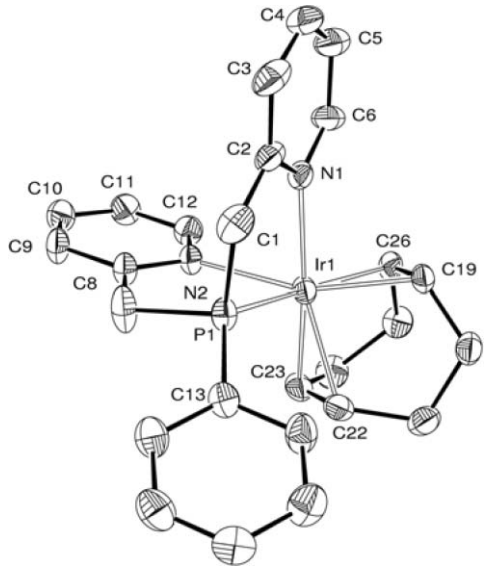

Fig. 6 ORTEP of the cationic complex in **7** with ellipsoids drawn at the 30% probability level. Selected bond distances (Å) and angles (deg): Ir1–N1 2.150(5), Ir1–N2 2.274(5), Ir1–P1 2.277(2), Ir1–C22/23 2.032(4), Ir1–C19/26 1.992(4), C22–C23 1.398(10), C19–C26 1.443(9), N1–Ir1–N2 83.9(2), N1–Ir1–P1 81.0(2), N2–Ir1–P1 79.0(1), C22/23–Ir1–C16/C26 85.5(3).

characterized iridium compounds bearing a chelated *N*,*P*,*N*-ligand have been reported to date.[29,37]

The 1 : 2 reaction between the iridium(I) precursor [Ir(μ-Cl)(cod)]$_2$ and $N_{py}PN_{py}$ afforded an air-sensitive orange compound in high yield. Although the attempts to get crystals suitable for X-ray diffraction failed, the formation of a new complex of formula [IrCl(cod)($N_{py}PN_{py}$)] (**6**) was inferred from spectroscopic and elemental analysis data. The coordination of the $N_{py}PN_{py}$ ligand through its phosphorus atom was demonstrated by the $^{31}P\{^1H\}$ NMR spectrum in $CDCl_3$, which consists in a sharp singlet at 24.7 ppm, 30 ppm downfield shifted with respect to the free ligand. Differently from that observed for compounds **1–3**, all the signals in the ^1H NMR spectrum of **6** are sharp. Moreover, four sharp signals in the pyridine region and only one ABX spin system in the CH_2 region were detected. These observations are consistent with a tridentate behaviour of the $N_{py}PN_{py}$ ligand, whose picolyl moieties would be symmetrically coordinated to the metal centre. As shown in Scheme 7 and Fig. 6, the two *P*,*N*-chelating arms are not equivalent and the fact that only one ABX spin system due to the CH_2P protons is observed (two doublets of doublets at 5.01 and 3.77 ppm with $^2J_{HH}$ = 17.6 Hz and $^3J_{PH}$ = 13.5 and 9.7 Hz) could be due to rapid exchange or to an equilibrium between a trigonal bipyramidal and a square-base pyramidal coordination geometry that would render the two P,N arms equivalent. Three resonances between 3.50 and 1.80 ppm are due to the coordinated cod ligand. In particular, the protons of the methylene groups of the cyclooctadiene become non-equivalent upon coordination and give rise to two multiplets. The $^{13}C\{^1H\}$ NMR spectrum of **6** displays two doublets at 63.0 ($^2J_{PC}$ = 8.7 Hz) and 33.0 ($^3J_{PC}$ = 1.8 Hz) ppm, attributed to the CH and the CH_2 carbons of the cod, respectively. IR spectroscopy was very useful to better understand the molecular structure of **6**. In particular, the far IR spectrum of the compound did not show any strong absorption around 300 cm^{-1} and this led us to rule out the presence of Ir–Cl bonds.[39] In agreement with the spectroscopic data and the elemental analysis, we propose that **6** is a penta-coordinated cationic complex. As far as the coordination environment of the metal is concerned, two different geometries have been reported for Ir(I) complexes

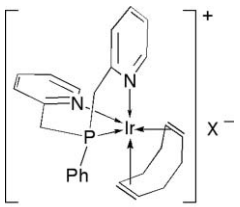

6 X = Cl
7 X = BAr^F

Scheme 7 Structures of **6** and **7** based on the X-ray diffraction structure of **7**.

containing cyclooctadiene and phosphine ligands, namely trigonal bipyramidal and square pyramidal.[40-42] In most of them, the metal centre lies in a distorted trigonal bipyramidal environment, the double bonds of the cod ligand occupying an equatorial and an apical position, as shown in Scheme 7.

It was hoped that the substitution of the chloride anion with a (tetra)arylborate would promote the crystallization of the complex and increase its solubility in solvents of low polarity. Therefore, we reacted [Ir(μ-Cl)(cod)]$_2$ with the $N_{py}PN_{py}$ ligand and added two equivalents of $NaBAr^F$ to the reaction mixture. The yellow crystalline product, which was isolated in high yield after removing the NaCl formed, was fully characterized by IR and NMR spectroscopic methods, elemental analysis, and X-ray diffraction, and identified as the cationic complex [Ir(cod)($N_{py}PN_{py}$-*N*,*P*,*N*)]BAr^F (**7**). Its $^{31}P\{^1H\}$ NMR spectrum in $CDCl_3$ displays a sharp singlet at 24.2 ppm, with a difference of only 0.5 ppm with respect to that of **6**. This suggests a very similar chemical environment around the phosphorus donor atom. With the exception of the signals due to the counteranion, the $^{13}C\{^1H\}$ NMR spectra of **6** and **7** are also very similar in terms of chemical shifts and coupling constants. The main difference between the ^1H NMR spectra of

6 and **7** concerns the ABX spin system due to the CH_2P protons. As previously mentioned, the two diastereotopic protons of **6** give rise to two doublets of doublets at 5.01 and 3.77 ppm. In the case of **7**, instead, they give rise to a multiplet between 3.90–3.80 ppm. By means of spectral simulation we could estimate the parameters of this ABX spin system as $\delta_A = 3.86$ ppm, $\delta_B = 3.84$ ppm, $^2J_{AB} = 18.4$ Hz, $^2J_{AX} = 2.6$ Hz and $^2J_{BX} = 19.6$ Hz. A view of the molecular structure of the cation $[Ir(cod)(N_{py}PN_{py})]^+$ of **7** in the solid state is shown in Fig. 6.

The coordination geometry around the metal is best described as trigonal bipyramidal. Two equatorial (P, N) and one apical (N) positions are occupied by the donor atoms of the $N_{py}PN_{py}$ ligand, which acts as a facial, tridentate *N*,*P*,*N*-donor. Similarly, in the octahedral Cr^{III} complex $[CrCl_3(N_{py}PN_{py}\text{-}N,P,N)]$ the ligand exhibits a facial coordination mode with the phosphorus atom in an apical position.[36] The two C=C double bonds of the cyclooctadiene complete the coordination sphere of the metal. The apical Ir–N bond (2.150(5) Å) is shorter than the equatorial one (2.274(5) Å).

Conclusions

New coordination complexes of Pd(II) and Ir(I) bearing the neutral ligand $N_{py}PN_{py}$ have been prepared in high yields from $[PdCl_2(NCPh)_2]$ or $[Ir(\mu\text{-}Cl)(cod)]_2$ and the ligand. The solid-state structures of the compounds (**1–5** and **7**) point out the versatility of the $N_{py}PN_{py}$ molecule, which can act as a *N*,*P*-chelating ligand (in **1** and **4**), *N*,*P*,*N*-*mer*-chelating ligand (in **2** and **5**), (*N*,*P*)-*N* chelating/bridging ligand (in **3**), *N*,*P*,*N*-*fac*-chelating ligand (in **7**). On the basis of NMR experiments in DMSO-d_6, the hemilability of $N_{py}PN_{py}$ in **1** has been demonstrated, the two pyridine moieties being involved in a dynamic exchange in the coordination sphere of the metal. Dynamic processes in DMSO solution have also been observed for complex **2** and an equilibrium between the species $[PdCl(N_{py}PN_{py}\text{-}N,P,N)]^+$ and $[PdCl(N_{py}PN_{py}\text{-}N,P)(DMSO)]^+$ has been inferred. The unexpected dinuclear compound **3** has been isolated as a by-product of the synthesis of its isomer **2**. We have also demonstrated that, in spite of the stability of **3** in the solid state, it can be converted into **2** in DMSO solution. A rational, stepwise preparation of **3** has been described, which involves the preparation of the dicationic complex *cis*-$[Pd(N_{py}PN_{py}\text{-}N,P)_2](BF_4)_2$ (**4**) and its reaction with $[PdCl_2(cod)]$. Interesting comparisons become thus possible between the palladium complexes of the related $N_{py}PN_{py}$ and $N_{ox}PN_{ox}$ ligands.[38] The Ir(I) cationic complex $[Ir(cod)(N_{py}PN_{py}\text{-}N,P,N)]BAr^F$ (**7**) is, to the best of our knowledge, only the third Ir(I) complex containing a *N*,*P*,*N*-chelating ligand to be structurally characterized.[29,37]

Experimental

General considerations

All operations were carried out using standard Schlenk techniques under an inert atmosphere. Solvents were dried, degassed, and freshly distilled prior to use. Et_2O and THF were dried over sodium/benzophenone. Pentane was dried over sodium. CH_2Cl_2 and acetonitrile were distilled from CaH_2. DMF, DMSO-d_6 and $CDCl_3$ were dried over 4 Å molecular sieves, degassed by freeze–pump–thaw cycles and stored under argon. Unless otherwise stated, NMR spectra were recorded at room temperature on a Bruker AVANCE 300 spectrometer (^1H, 300 MHz; ^{13}C, 75.47 MHz; ^{19}F, 282.4 MHz; ^{31}P, 121.5 MHz) or on a Bruker AVANCE 400 spectrometer (^1H, 400 MHz; ^{13}C, 100.60 MHz, ^{31}P, 162.0 MHz) and referenced using the residual proton solvent (^1H) or solvent (^{13}C) resonance. Assignments are based on DEPT135, COSY, HMQC and HMBC experiments. IR spectra were recorded in the region 4000–100 cm^{-1} on a Nicolet 6700 FT-IR spectrometer equipped with a Smart Orbit ATR accessory (Ge or diamond crystals). Elemental analyses were performed by the "Service de microanalyse", Université de Strasbourg. Yields of the complexes are based on the metal. $[Ir(\mu\text{-}Cl)(cod)]_2$ and $TlPF_6$ were purchased from UMICORE and Alfa Aesar and used as received. Bis(2-picolyl)phenylphosphine ($N_{py}PN_{py}$),[17] $[PdCl_2(NCPh)_2]$,[43] $Na[B(3,5\text{-}(CF_3)_2C_6H_3)_4]$,[44] $[Pd(NCMe)_4](BF_4)_2$,[45] and $[PdCl_2(cod)]$ [46] were prepared according to literature methods. Other chemicals were commercially available and used as received.

Synthesis of $[PdCl_2(N_{py}PN_{py})]$ (1). Solid $[PdCl_2(NCPh)_2]$ (0.722 g, 1.88 mmol) was added to a solution of $N_{py}PN_{py}$ (0.550 g, 1.88 mmol) in dichloromethane (20 mL) to give a yellow suspension, which was stirred overnight. The solvent was removed under vacuum affording a yellow powder which was washed with diethyl ether (2 × 20 mL) and dried *in vacuo* overnight (Yield: 0.697 g, 1.32 mmol, 79%). Selected IR absorptions (pure, diamond orbit): 1604 m, 1587 m, 1468 ms, 1436 s, 1107 m, 844 s, 803 s, 785 s, 744 s, 684 s, 337 m, 301 m cm^{-1}. $^1H\{^{31}P\}$ NMR (400.13 MHz, DMSO-d_6): δ 9.31 (br, 1H, py^6), 8.38 (br, 1H, py^6), 8.04 (br, 1H, py^4), 7.87 (d, 2H, $^3J_{HH} = 7.5$ Hz, *o*-aryl), 7.81 (br, 1H, py^3), 7.71 (br, 1H, py^4), 7.58 (t, 1H, $^3J_{HH} = 7.4$ Hz, *p*-aryl), 7.51–7.35 (m, 4H, *m*-aryl, py^5 and py^3), 7.24 (br, 1H, py^5), 4.70 and 4.25 (AB spin system, 2H, $^2J_{HH} = 16.4$ Hz, CH_2), 4.25 and 4.08 (AB spin system, 2H, $^2J_{HH} = 14.4$ Hz, CH_2) ppm. $^{13}C\{^1H\}$ NMR (75.5 MHz, DMSO-d_6): δ 162.5 (s, coordinated py^2), 153.4 (s, uncoordinated py^2), 152.2 (s, coordinated py^6), 149.6 (s, uncoordinated py^6), 140.8 (s, coordinated py^4), 137.5 (s, uncoordinated py^4), 132.6 (s, *p*-aryl), 132.2 (d, $^2J_{PC} = 10.0$ Hz, *o*-aryl), 129.5 (d, $^3J_{PC} = 11.2$ Hz, *m*-aryl), 127.7 (d, $^1J_{PC} = 52.2$ Hz, *ipso*-aryl), 125.7 (s, py), 124.8 (s, py), 124.1 (s, py), 122.9 (s, py), coordinated CH_2 partially masked by the solvent resonance, 34.8 (d, $^1J_{PC} = 31.3$ Hz, uncoordinated CH_2) ppm. $^{31}P\{^1H\}$ NMR (121.5 MHz, DMSO-d_6): δ 49.7 (s) ppm. Anal. Calcd for $C_{18}H_{17}Cl_2N_2PPd$: C, 46.03; H, 3.65; N, 5.96. Found: C, 45.53; H, 3.83; N, 5.86. Crystals suitable for X-ray diffraction were grown by slow cooling of a concentrated solution of the pure compound in DMF.

Synthesis of $[PdCl(N_{py}PN_{py})]PF_6$ (2) and $[Pd_2Cl_2(\mu\text{-}N_{py}PN_{py})_2](PF_6)_2$ (3). Solid $[PdCl_2(NCPh)_2]$ (0.690 g, 1.80 mmol) was added to a solution of $N_{py}PN_{py}$ (0.525 g, 1.80 mmol) in THF (20 mL) to give a yellow suspension, which was stirred overnight. $TlPF_6$ (0.629 g, 1.80 mmol) was added and the mixture was stirred for 12 h. The solvent was removed by evaporation under reduced pressure and the solid residue was extracted in DMF and the solution was filtered to remove TlCl. Et_2O was added and a yellow solid separated out which was shown by ^1H NMR to contain two products (see text). After filtration and washing of the yellow solid with CH_2Cl_2 (3 × 10 mL), the combined filtrates were concentrated to 10 mL under reduced pressure to give yellow crystals of $[Pd_2Cl_2(\mu\text{-}N_{py}PN_{py})_2](PF_6)_2$,

suitable for X-ray diffraction (0.100 g, 0.086 mmol, 10% yield based on Pd). The insoluble pale yellow residue was identified as $[PdCl(N_{py}PN_{py})]PF_6$ (0.762 g, 1.32 mmol, 73%). Selected IR absorptions (pure, diamond orbit) for $[PdCl(N_{py}PN_{py})]PF_6$: 1666w, 1606w, 1474w, 1439w, 1110w, 835vs, 768 m, 688 m, 556 s, 343 m cm^{-1}. The following NMR data correspond to the sharp signals of the cationic complex $[PdCl(NPN)]^+$. ^1H NMR (300.13 MHz, DMSO-d_6): δ 9.06 (d, 2H, $^3J_{HH}$ = 4.9 Hz, py^6), 8.25–8.20 (m, 2H, py^4), 7.99–7.90 (m, 4H, py^3 and *o*-aryl), 7.68-7.51 (m, 5H, py^5, *p*- and *m*-aryl), 5.30–5.19 (m, 2H, $^2J_{HH} \approx {}^2J_{PH} \approx$ 17.3 Hz, C*H*H), 4.39–4.23 (m, 2H, $^2J_{HH} \approx {}^2J_{PH} \approx$ 17.3 Hz, CH*H*) ppm. $^{13}C\{^1H\}$ NMR (75.5 MHz, DMSO-d_6): δ 164.9 (s, py^2), 153.6 (s, py^6), 142.0 (s, py^4), 133.9–124.9 (m, py^{3,5} and aryl), 38.5 (d, $^1J_{PC}$ = 36.7 Hz, CH_2) ppm. $^{31}P\{^1H\}$ NMR (121.5 MHz, DMSO-d_6): δ 83.7 (br, $N_{py}PN_{py}$), –143.0 (sept, $^1J_{PF}$ = 712 Hz, PF_6^-) ppm. Anal. Calcd for $C_{18}H_{17}ClF_6N_2P_2Pd$: C, 37.33; H, 2.96; N, 4.84. Found: C, 37.55; H, 3.06; N, 4.82. Crystals suitable for X-ray diffraction were grown by cooling a hot dichloromethane solution of the pure compound to room temperature.

$[Pd_2Cl_2(\mu\text{-}N_{py}PN_{py})_2](PF_6)_2$ (3). Selected IR absorptions (pure, diamond orbit): 1606 w, 1572 w, 1476 w, 1437 w, 1102 m, 836 vs, 759 m, 746 m, 694 m, 555 s, 346 m cm^{-1}. ^1H NMR (300.13 MHz, DMSO-d_6): δ 9.27 (d, 2H, $^3J_{HH}$ = 5.4 Hz, py^6), 8.20–8.17 (m, 2H, py), 8.10-8.05 (m, 2H, py^4), 7.98–7.93 (m, 2H, py), 7.78–7.67 (m, 8H, py and *o*-aryl), 7.60–7.51 (m, 6H, py and *p*-aryl), 7.40–7.34 (m, 4H, *m*-aryl), 5.66 (br, 2H, CH_2), 4.77–4.30 (m, 4H, CH_2), 3.94 (br, 2H, CH_2) ppm. $^{31}P\{^1H\}$ NMR (121.5 MHz, DMSO-d_6): δ 47.5 (br, $N_{py}PN_{py}$), –143.0 (sept, $^1J_{PF}$ = 712 Hz, PF_6^-) ppm. We could not record the $^{13}C\{^1H\}$ NMR spectrum of the pure compound because it isomerises slowly to the monomer in DMSO solution. Anal. Calcd for $C_{18}H_{17}ClF_6N_2P_2Pd$: C, 37.33; H, 2.96; N, 4.84. Found: C, 37.21; H, 3.17; N, 4.72.

Synthesis of $[Pd(N_{py}PN_{py})_2](BF_4)_2$ (4). Solid $[Pd(NCCH_3)_4](BF_4)_2$ (0.222 g, 0.50 mmol) was added to a solution of $N_{py}PN_{py}$ (0.292 g, 1.00 mmol) in dichloromethane (20 mL). The resulting yellow suspension was stirred overnight at room temperature. The solvent was concentrated to 5 mL under reduced pressure affording a pale yellow powder, which was washed with diethyl ether (2 × 20 mL) and dried *in vacuo* overnight (Yield: 0.337 g, 0.39 mmol, 78%). Selected IR absorptions (pure, diamond orbit): 1605 w, 1588 w, 1571 w, 1473 m, 1437 m, 1397 w, 1315 m, 1162 m, 1028 vs, 888 s, 833 m, 752 s, 692 s cm^{-1}. ^1H NMR (300.13 MHz, DMSO-d_6): δ 8.23 (d, 4H, $^3J_{HH}$ = 5.2 Hz, py^6), 7.80 (t, 4H, $^3J_{HH}$ = 7.7 Hz, py^4), 7.71–7.64 (m, 6H, *p*- and *o*-aryl), 7.52–7.45 (m, 8H, py^3 and *m*-aryl), 7.30 (t, 4H, py^5), 4.31–4.14 (m, 8H, CH_2) ppm. $^{13}C\{^1H\}$ NMR (75.5 MHz, DMSO-d_6): δ 155.7 (s, py^2), 150.6 (s, py^6), 139.7 (s, py^4), 133.7 (s, *p*-aryl), 132.4 (d, $^2J_{PC}$ = 11.1 Hz, *o*-aryl), 129.7 (d, $^3J_{PC}$ = 11.8 Hz, *m*-aryl), 125.2 (d, $^1J_{PC}$ = 56.3 Hz, *ipso*-aryl), 125.2 (d, $^3J_{PC}$ = 9.3, py^3), 124.1 (s, py^5), 36.7 (d, $^1J_{PC}$ = 30.2 Hz, CH_2) ppm. $^{31}P\{^1H\}$ NMR (121.5 MHz, DMSO-d_6): δ 47.0 (s) ppm. Anal. Calcd for $C_{36}H_{34}B_2F_8N_4P_2Pd$ C, 50.01; H, 3.96 N, 6.48. Found: C, 49.97; H, 3.86; N, 6.49. Crystals suitable for X-ray diffraction were grown by layering Et_2O on a concentrated dichloromethane solution of the pure compound.

Synthesis of $[Pd(N_{py}PN_{py})(MeCN)](PF_6)_2$ (5). Solid $[PdCl_2(NCPh)_2]$ (0.384 g, 1.00 mmol) was added to a solution of $N_{py}PN_{py}$ (0.290 g, 1.00 mmol) in acetonitrile (20 mL). The yellow suspension was stirred overnight, $TlPF_6$ (0.698 g, 2.00 mmol) was then added and the mixture was further stirred for 12 h. After filtration and washing of the solid residue with acetonitrile (3 × 10 mL), the combined filtrates were concentrated to 5 mL, and Et_2O (20 mL) was added affording the precipitation of pure $[Pd(N_{py}PN_{py})(NCMe)](PF_6)_2$ as a pale yellow solid (Yield: 0.584 g, 0.80 mmol, 80%). Selected IR absorptions (pure, diamond orbit): 1609 w, 1476 w, 1437 w, 1111 m, 832 vs, 776 m, 742 m, 689 m, 554 s cm^{-1}. $^1H\{^{31}P\}$ NMR (400.13 MHz, DMSO-d_6): δ 8.51 (d, 2H, $^3J_{HH}$ = 5.4 Hz, py^6), 8.26 (td, 2H, $^3J_{HH}$ = 7.9 Hz, $^4J_{HH}$ = 1.5 Hz, py^4), 8.00 (d, $^3J_{HH}$ = 7.9 Hz, 2H, py^3), 7.70–7.67 (m, 3H, py^5 and *p*-aryl), 7.64–7.62 (m, 2H, *o*-aryl), 7.55–7.51 (m, 2H, *m*-aryl), 5.21 and 4.29 (AB spin system, $^2J_{HH}$ = 17.7 Hz, 4H, CH_2), 2.07 (s, 3H, free CH_3CN) ppm. $^{13}C\{^1H\}$ NMR (75.5 MHz, DMSO-d_6): δ 164.0 (s, py^2), 151.6 (s, py^6), 142.4 (s, py^4), 134.1 (d, $^4J_{PC}$ = 2.6 Hz, *p*-aryl), 131.7 (d, $^2J_{PC}$ = 11.2 Hz, *o*-aryl), 130.4 (d, $^3J_{PC}$ = 12.7 Hz, *m*-aryl), 126.3 (d, $^3J_{PC}$ = 15.3 Hz, py^3), 125.7 (s, py^5), 124.4 (d, $^1J_{PC}$ = 58.6 Hz, *ipso*-aryl), 118.5 (s, free CH_3CN), CH_2 partially masked by the solvent resonance, 1.5 (s, free CH_3CN). $^{31}P\{^1H\}$ NMR (121.5 MHz, DMSO-d_6): δ 86.6 (s, $N_{py}PN_{py}$), –143.0 (sept, $^1J_{PF}$ = 712 Hz, PF_6^-) ppm. Anal. Calcd for $C_{20}H_{20}F_{12}N_3P_3Pd{\cdot}CH_3CN$: C, 34.28; H, 3.01; N, 7.27. Found: C, 34.21; H, 3.17; N, 6.98. Crystals suitable for X-ray diffraction were grown by layering Et_2O on a concentrated acetonitrile solution of the pure compound.

Synthesis of $[IrCl(cod)(N_{py}PN_{py})]$ (6). Solid $[Ir(\mu\text{-}Cl)(cod)]_2$ (0.260 g, 0.387 mmol) was added to a solution of the $N_{py}PN_{py}$ ligand (0.220 g, 0.787 mmol) in CH_2Cl_2 (10 mL). The orange solution was stirred for 1 h. The solvent was evaporated under reduced pressure to give an orange solid, which was washed with pentane (2 × 5 mL) and dried *in vacuo* (Yield: 0.430 g, 0.684 mmol, 88%). Selected IR absorptions (pure, diamond orbit): 1597 m, 1472 ms, 1435 ms, 1106 ms, 1011 m, 744 s, 695 s cm^{-1}. ^1H NMR (300.13 MHz, $CDCl_3$): δ 8.76 (dd, 2H, $^3J_{HH}$ = 5.6 Hz, $^4J_{HH}$ = 1.0 Hz, py^6), 7.92–7.85 (m, 2H, *o*-aryl), 7.79 (d, 2H, $^3J_{HH}$ = 7.9 Hz, py^3), 7.70–7.62 (m, 2H, py^4), 7.59–7.47 (m, 3H, *m*-, *p*-aryl), 7.14–7.06 (m, 2H, py^5), 5.01 and 3.77 (ABX spin system, 4H, $^2J_{HH}$ = 17.6 Hz, $^2J_{PH}$ = 13.5 Hz and 9.7 Hz, PCH_2), 3.40 (s, 4H, CH cod), 2.40–2.20 (m, 4H, CH_2 cod), 1.95–1.75 (m, 4H, CH_2 cod) ppm. $^{13}C\{^1H\}$ NMR (75.5 MHz, $CDCl_3$): δ 161.9 (d, $^2J_{PC}$ = 6.2 Hz, py^6), 150.7 (d, $^3J_{PC}$ = 3.5 Hz, py^2), 138.3 (s, py^4), 131.9 (d, $^2J_{PC}$ = 11.2 Hz, *o*-aryl), 131.3 (d, $^4J_{PC}$ = 2.3 Hz, *p*-aryl), 129.4 (d, $^3J_{PC}$ = 10.6 Hz, *m*-aryl), 126.6 (d,$^1J_{PC}$ = 49.7 Hz, *ipso*-aryl), 125.4 (d, $^3J_{PC}$ = 9.7 Hz, py^3), 123.9 (s, py^5), 63.0 (d, $^2J_{PC}$ = 8.7 Hz, CH cod), 41.8 (d, $^2J_{PC}$ = 28.7 Hz, CH_2P), 33.0 (d, $^3J_{PC}$ = 1.8 Hz, CH_2 cod) ppm. $^{31}P\{^1H\}$ NMR (121.5 MHz, $CDCl_3$): δ 24.7 (s) ppm. Anal. Calcd for $C_{26}H_{29}ClIrN_2P$: C, 49.71; H, 4.65; N, 4.46. Found: C, 49.76; H, 4.93; N, 4.12.

Synthesis of $[Ir(cod)(N_{py}PN_{py})]BAr^F$ (7). Solid $[Ir(\mu\text{-}Cl)(cod)]_2$ (0.160 g, 0.238 mmol) was added to a solution of the $N_{py}PN_{py}$ ligand (0.142 g, 0.486 mmol) in CH_2Cl_2 (10 mL). The orange solution was stirred for 1 h and then $NaBAr^F$ was added. The resulting yellow mixture was stirred overnight and filtered to remove NaCl. The solvent was removed under reduced pressure and the resulting yellow powder was washed with pentane (2 × 5 mL) and dried *in vacuo* (Yield: 0.440 g, 0.302 mmol, 63%). Crystals suitable for X-ray diffraction were grown by layering Et_2O and pentane on a concentrated solution of the compound

Table 1 Crystal data and X-ray refinement details for complexes **1**, [$PdBr_2(N_{py}PN_{py}$-*N*,*P*)], **2**·CH_2Cl_2, **3**·2(CH_2Cl_2), **4**·2(CH_2Cl_2), **5**·NCMe and **7**

	1	[$PdBr_2(N_{py}PN_{py}$-*N*,*P*)]	**2**·CH_2Cl_2	**3**·2(CH_2Cl_2)	**4**·2(CH_2Cl_2)	**5**·NCMe	**7**
Formula	$C_{18}H_{17}Cl_2N_2PPd$	$C_{18}H_{17}Br_2N_2PPd$	$C_{18}H_{17}ClF_6N_2P_2Pd\cdot CH_2Cl_2$	$C_{36}H_{34}Cl_2F_{12}N_4P_4Pd_2\cdot 2(CH_2Cl_2)$	$C_{36}H_{34}B_2F_8N_4P_2Pd\cdot 2(CH_2Cl_2)$	$C_{20}H_{20}F_{12}N_3P_3Pd\cdot C_2H_3N$	$C_{58}H_{41}BF_{24}IrN_2P$
M_r/g mol^{-1}	469.61	558.53	664.05	1328.10	1034.48	770.75	1455.91
Crystal system	Monoclinic	Monoclinic	Monoclinic	Triclinic	Monoclinic	Monoclinic	Triclinic
Space group	$C2/c$	$C2/c$	$P2_1/c$	$P\bar{1}$	$C2/c$	$P2_1/c$	$P\bar{1}$
a/Å	15.2170(5)	15.3788(5)	8.3181(3)	11.4281(2)	18.0622(6)	10.0969(5)	12.5163(3)
b/Å	13.7873(6)	14.0532(6)	13.5499(7)	14.2341(5)	10.3296(3)	33.8250(9)	14.9159(4)
c/Å	18.4593(7)	18.7832(5)	22.3438(9)	16.4503(5)	23.7608(9)	8.5479(4)	16.5224(4)
α (°)	90.00	90.00	90.00	92.746(2)	90.00	90.00	85.787(1)
β (°)	109.818(2)	110.209(2)	104.103(2)	101.798(2)	94.187(2)	101.223(2)	77.882(1)
γ (°)	90.00	90.00	90.00	108.351(2)	90.000	90.000	73.919(1)
V/Å^3	3643.4(2)	3809.5(2)	2442.45(18)	2467.99(12)	4421.3(3)	2863.5(2)	2897.47(13)
Z	8	8	4	2	4	4	2
Crystal size/mm	0.07 × 0.07 × 0.05	0.2 × 0.2 × 0.1	0.10 × 0.06 × 0.04	0.12 × 0.07 × 0.07	0.1 × 0.08 × 0.08	0.10 × 0.08 × 0.08	0.12 × 0.10 × 0.09
D_c/g cm^{-3}	1.712	1.948	1.806	1.787	1.554	1.788	1.669
μ/mm^{-1}	1.40	5.27	1.28	1.26	0.801	0.915	2.45
θmax/°	30.03	29.13	27.00	27.50	26.00	27.12	27.46
F(000)	1872	2160	1312	1312	2080	1528	1432
No. data measured	8415	8424	8909	16163	7367	26846	35209
No. data with $I > 2\sigma(I)$	3621	4094	3101	8171	3379	4424	9476
No. of variables	217	217	298	595	267	381	766
Final R indices [$I > 2\sigma(I)$]	$R_1 = 0.0427$ $wR_2 = 0.0978$	$R_1 = 0.0317$ $wR_2 = 0.0765$	$R_1 = 0.0516$ $wR_2 = 0.1186$	$R_1 = 0.0444$ $wR_2 = 0.1071$	$R_1 = 0.0511$ $wR_2 = 0.1430$	$R_1 = 0.0520$ $wR_2 = 0.1348$	$R_1 = 0.0558$ $wR_2 = 0.1342$
R indices all data	$R_1 = 0.0792$ $wR_2 = 0.1232$	$R_1 = 0.0486$ $wR_2 = 0.1026$	$R_1 = 0.1160$ $wR_2 = 0.1482$	$R_1 = 0.0734$ $wR_2 = 0.1304$	$R_1 = 0.0737$ $wR_2 = 0.1621$	$R_1 = 0.0841$ $wR_2 = 0.1552$	$R_1 = 0.0924$ $wR_2 = 0.1651$
GOF on F^2	1.049	1.143	0.959	1.079	1.085	1.041	1.035
Largest diff. peak, hole/e Å^{-3}	1.32, −1.26	0.72, −1.18	1.36, −1.26	0.98, −1.28	1.25, −1.02	1.20, −1.39	1.59, −1.65

in CH_2Cl_2. Selected IR absorptions (pure, diamond orbit): 1608 w, 1571 mw, 1354 m, 1277 vs, 1159 s, 1120 vs cm^{-1}. ^1H NMR (300.13 MHz, $CDCl_3$): 8.86 (d, 2H, $^3J_{HH} = 4.8$ Hz, py[6]), 7.80–7.66 (m, 10H, *o*-aryl, *o*-BAr^F), 7.64–7.58 (m, 3H, *p*-, *m*-aryl), 7.57–7.44 (m, 6H, py[4], *p*-BAr^F), 7.34 (d, 2H, $^3J_{HH} = 7.8$ Hz, py[3]), 7.08 (t, 2H, $^3J_{HH} = 6.2$ Hz, py[5]), 3.90–3.80 (m, ABX spin system, 4H, values from spectral simulation: $^2J_{HH} = 18.4$ Hz, $^2J_{PH} = 19.6$ Hz and 2.6 Hz, PCH_2), 3.46 (s, 4H, CH cod), 2.40–2.25 (m, 4H, CH_2 cod), 1.98-1.88 (m, 4H, CH_2 cod) ppm. $^{13}C\{^1H\}$ NMR (75.5 MHz, $CDCl_3$): δ 161.7 (q, $^1J_{BC} = 49.8$ Hz, *ipso*-aryl BAr^F), 160.2 (d, $^2J_{PC} = 7.3$ Hz, py[2]), 151.6 (d, $^3J_{PC} = 4.1$ Hz, py[6]), 138.7 (s, py[4]), 134.8 (s, *o*-aryl BAr^F), 132.2 (d, $^4J_{PC} = 2.6$ Hz, *p*-aryl), 131.0 (d, $^2J_{PC} = 11.3$ Hz, *o*-aryl), 129.9 (d, $^3J_{PC} = 10.7$ Hz, *m*-aryl), 128.9 (qq, $^2J_{CF} = 31.5$ Hz, $^3J_{BC} = 2.8$ Hz, CCF_3), 124.7 (s, py[5]), *ipso*-aryl masked, 124.5 (q, $^1J_{CF} = 272.5$ Hz, CF_3), 124.0 (d, $^3J_{PC} = 9.5$ Hz, py[3]), 117.5 (sept, $^3J_{CF} = 3.8$ Hz, *p*-aryl BAr^F), 64.3 (d, $^2J_{PC} = 8.7$ Hz, CH cod), 42.8 (d, $^2J_{PC} = 27.4$ Hz, CH_2P), 32.9 (d, $^2J_{PC} = 1.8$ Hz, CH_2 cod) ppm. $^{31}P\{^1H\}$ NMR (121.5 MHz, $CDCl_3$): δ 24.2 (s) ppm. ^{19}F NMR (282.4 MHz, $CDCl_3$): –62.8 ppm. Anal. Calcd for $C_{58}H_{41}BF_{24}IrN_2P$: C, 47.85; H, 2.84; N, 1.92. Found: C, 47.89; H, 2.86; N, 1.82.

Determination of the crystal structures

Diffraction data were collected at 173(2) K, on a Kappa CCD diffractometer using graphite-monochromated Mo-Kα radiation ($\lambda = 0.71073$ Å) (Table 1).[47] The structures were solved by direct methods using the SHELX 97 software,[47] and the refinement was by full-matrix least squares on F^2. A MULTISCAN absorption correction was applied on [$PdBr_2(N_{py}PN_{py}$-*N*,*P*)] and **7**.[48] All non-hydrogen atoms were refined anisotropically. The hydrogen atoms were introduced into the geometrically calculated positions (SHELXS-97 procedures) and refined *riding* on the corresponding parent atoms. In **7**, six CF_3 groups of the anion were found disordered. These groups were refined as disordered in two positions having the carbon atom in common, and with constrained anisotropic parameters.

Acknowledgements

We thank the Centre National de la Recherche Scientifique (CNRS), the Ministère de l'Enseignement Supérieur et de la Recherche (Paris) and the Université de Strasbourg for support, the French Embassy in Beijing for a doctoral grant to S. L. and Professor Wen-Hua Sun (Institute of Chemistry, Chinese Academy of Sciences, Beijing) for support. We are grateful to Drs Lydia Brelot (X-ray structure analyses) and Roberto Pattacini (X-ray structure analyses and discussions), Dr Weiwei Zuo for experimental assistance, and Dr Joaquín López-Serrano for helpful discussions on NMR analyses.

Notes and references

1 G. Helmchen and A. Pfaltz, *Acc. Chem. Res.*, 2000, **33**, 336.
2 P. Braunstein and F. Naud, *Angew. Chem., Int. Ed.*, 2001, **40**, 680.
3 D. Rechavi and M. Lemaire, *Chem. Rev.*, 2002, **102**, 3467.
4 H. A. McManus and P. J. Guiry, *Chem. Rev.*, 2004, **104**, 4151.
5 G. Desimoni, G. Faita and K. A. Jøensen, *Chem. Rev.*, 2006, **106**, 3561.
6 P. Braunstein, C. Graiff, F. Naud, A. Pfaltz and A. Tiripicchio, *Inorg. Chem.*, 2000, **39**, 4468.
7 F. Speiser, P. Braunstein and L. Saussine, *Acc. Chem. Res.*, 2005, **38**, 784.
8 J. Hou, W.-H. Sun, S. Zhang, H. Ma, Y. Deng and X. Lu, *Organometallics*, 2006, **25**, 236.
9 P. Braunstein, *Chem. Rev.*, 2006, **106**, 134.
10 S. Maggini, *Coord. Chem. Rev.*, 2009, **253**, 1793.
11 P. Espinet and K. Soulantica, *Coord. Chem. Rev.*, 1999, **193–195**, 499.
12 P. Braunstein, M. D. Fryzuk, F. Naud and S. J. Rettig, *J. Chem. Soc., Dalton Trans.*, 1999, 589.
13 P. Braunstein, F. Naud, A. Pfaltz and S. J. Rettig, *Organometallics*, 2000, **19**, 2676.
14 P. Braunstein, F. Naud, C. Graiff and A. Tiripicchio, *Chem. Commun.*, 2000, 897.
15 P. Braunstein, F. Naud and S. J. Rettig, *New J. Chem.*, 2001, **25**, 32.
16 A. Kermagoret and P. Braunstein, *Organometallics*, 2008, **27**, 88.
17 A. Kermagoret, F. Tomicki and P. Braunstein, *Dalton Trans.*, 2008, 2945.
18 S. Jie, M. Agostinho, A. Kermagoret, C. S. J. Cazin and P. Braunstein, *Dalton Trans.*, 2007, 4472.
19 P. Braunstein, M. D. Fryzuk, M. Le Dall, F. Naud, S. Rettig and F. Speiser, *J. Chem. Soc., Dalton Trans.*, 2000, 1067.
20 M. Agostinho, P. Braunstein and R. Welter, *Dalton Trans.*, 2007, 759.
21 P. Braunstein, G. Clerc and X. Morise, *New J. Chem.*, 2003, **27**, 68.
22 P. Braunstein, G. Clerc, X. Morise, R. Welter and G. Mantovani, *Dalton Trans.*, 2003, 1601.
23 A. Kermagoret and P. Braunstein, *Dalton Trans.*, 2008, 585.
24 F. Hung-Low, A. Renz and K. K. Klausmeyer, *Eur. J. Inorg. Chem.*, 2009, 2994.
25 E. Lindner, H. Rauleder and W. Hiller, *Z. Naturforsch., B: Anorg. Chem. Org. Chem.*, 1983, **38B**, 417.
26 C. Slugovc, I. Padilla-Martinez, S. Sirol and E. Carmona, *Coord. Chem. Rev.*, 2001, **213**, 129.
27 A. S. Goldman, A. H. Roy, Z. Huang, R. Ahuja, W. Schinski and M. Brookhart, *Science*, 2006, **312**, 257.
28 M. T. Whited, Y. Zhu, S. D. Timpa, C.-H. Chen, B. M. Foxman, O. V. Ozerov and R. H. Grubbs, *Organometallics*, 2009, **28**, 4560.
29 R. Peloso, R. Pattacini, C. S. J. Cazin and P. Braunstein, *Inorg. Chem.*, 2009, **48**, 11415.
30 W. Linert, Y. Fukuda and A. Camart, *Coord. Chem. Rev.*, 2001, **218**, 113.
31 M. Pfeffer, P. Braunstein and J. Dehand, *Spectrochim. Acta, Part A*, 1974, **30A**, 341.
32 P.-C. Kong and F. D. Rochon, *Can. J. Chem.*, 1981, **59**, 3293.
33 P. Braunstein, F. Naud, A. Dedieu, M.-M. Rohmer, A. DeCian and S. J. Rettig, *Organometallics*, 2001, **20**, 2966.
34 T. G. Appleton, H. C. Clark and L. E. Manzer, *Coord. Chem. Rev.*, 1973, **10**, 335.
35 H. Morita, S. Shimomura and S. Kawaguchi, *Bull. Chem. Soc. Jpn.*, 1979, **52**, 1838.
36 K. K. Klausmeyer and F. Hung, *Acta Crystallogr., Sect. E: Struct. Rep. Online*, 2006, **E62**, m2415.
37 J. A. Camerano, M. A. Casado, M. A. Ciriano, C. Tejel and L. A. Oro, *Chem.–Eur. J.*, 2008, **14**, 1897.
38 J. Zhang, R. Pattacini and P. Braunstein, *Inorg. Chem.*, 2009, **48**, 11954.
39 K. D. Schramm, T. H. Tulip and J. A. Ibers, *Inorg. Chem.*, 1980, **19**, 3183.
40 M. R. Churchill and S. A. Bezman, *Inorg. Chem.*, 1972, **11**, 2243.
41 M. R. Churchill and S. A. Bezman, *Inorg. Chem.*, 1973, **12**, 260.
42 J. F. Frazier and J. S. Merola, *Polyhedron*, 1992, **11**, 2917.
43 G. K. Anderson and M. Lin, *Inorg. Synth.*, 1990, **28**, 60.
44 N. A. Yakelis and R. G. Bergman, *Organometallics*, 2005, **24**, 3579.
45 B. B. Wayland and R. F. Schramm, *Inorg. Chem.*, 1969, **8**, 971.
46 F. R. Hartley, *The chemistry of Platinum and Palladium*, Elsevier, Amsterdam, 1973.
47 Bruker-Nonius, *Kappa CCD Reference Manual*, Nonius BV, The Netherlands, 1998; G. M. Sheldrick, *SHELXL97, Program for the refinement of crystal structures*, University of Göttingen, Germany, 1997.
48 L. Spek, *J. Appl. Crystallogr.*, 2003, **36**, 7; B. Blessing, *Acta Crystallogr., Sect. A: Found. Crystallogr.*, 1995, **A51**, 33.

